

2006

# High temperature ferromagnetism in Ni-doped In<sub>2</sub>O<sub>3</sub> and indium-tin oxide

G. Peleckis

*University of Wollongong*

X. L. Wang

*University of Wollongong, xiaolin@uow.edu.au*

S. X. Dou

*University of Wollongong, shi\_dou@uow.edu.au*

---

## Publication Details

This article was originally published as: Peleckis, G, Wang, X & Dou, S, High temperature ferromagnetism in Ni-doped In<sub>2</sub>O<sub>3</sub> and indium-tin oxide, *Applied Physics Letters*, 89(2), 2006, 022501. Original journal available [here](#).

## High temperature ferromagnetism in Ni-doped $\text{In}_2\text{O}_3$ and indium-tin oxide

Germanas Peleckis, Xiaolin Wang,<sup>a)</sup> and Shi Xue Dou

*Institute for Superconducting and Electronic Materials, University of Wollongong, Wollongong, New South Wales 2522, Australia*

(Received 7 February 2006; accepted 22 May 2006; published online 10 July 2006)

Observation of high temperature ferromagnetism in Ni-doped  $\text{In}_2\text{O}_3$  and indium-tin-oxide (ITO) samples prepared by a solid state synthesis route is reported. Both Ni-doped compounds showed a clear ferromagnetism above 300 K with the magnetic moments of  $0.03\text{--}0.06\mu_B/\text{Ni}$  and  $0.1\mu_B/\text{Ni}$  at 300 and 10 K, respectively. Ni-doped  $\text{In}_2\text{O}_3$  samples showed a typical semiconducting behavior with a room temperature resistivity of  $\rho \sim 2 \Omega \text{ cm}$ , while Ni-doped ITO samples were metallic with  $\rho \sim 2 \times 10^{-2} \Omega \text{ cm}$ . Analysis of different conduction mechanisms suggested that variable range hopping model explains our  $\rho$ - $T$  data for the Ni-doped  $\text{In}_2\text{O}_3$  sample the best. © 2006 American Institute of Physics. [DOI: 10.1063/1.2220529]

Since the discovery of the giant magnetoresistance (GMR) effect in metallic multilayer structures,<sup>1</sup> much effort has been put into developing and finding new materials that utilize the spin of electrons. Usually diluted magnetic semiconductors (DMSs) are formed when magnetic transition metal ions, such as  $3d$  elements, are doped into the host lattice of a semiconductor. Theoretical predictions by Dietl *et al.*<sup>2</sup> have boosted the search for ferromagnetism in the transition metal doped ZnO. The obtained results are very controversial, where some groups claimed that this system is ferromagnetic,<sup>3–5</sup> while others have found no ferromagnetism in TM doped ZnO.<sup>6–8</sup> Recently, high temperature ferromagnetism was observed in Co-doped  $\text{SnO}_2$  with large magnetic moment  $\sim 7.5\mu_B/\text{Co}$ .<sup>9</sup> However, this giant magnetic moment was found only in as prepared samples. Due to the small solubility of magnetic ions in the host semiconductor, ferromagnetism probably is induced by the clusters of dopants formed during the sample preparation procedure.<sup>10</sup>

If one considers integrating electronic, magnetic, and photonic properties in the new generation devices, the materials suitable for such devices should have high tunability of charge carriers, high carrier mobility, optical transparency, high abundance of the consisting elements, and low impact on the environment.  $\text{In}_2\text{O}_3$  is one of the most promising candidates for such tasks. It is a well known semiconducting oxide already used practically worldwide. When  $\text{In}_2\text{O}_3$  is doped with Sn, a so called indium-tin oxide (ITO) is formed. High conductivity of ITO is attributed to the high carrier concentration which is caused by incorporation of Sn ions into  $\text{In}_2\text{O}_3$  host lattice and oxygen nonstoichiometry. ITO has a cubic bixbyite structure with the lattice parameter  $a = 10.118 \text{ \AA}$ .<sup>11</sup> Electrical conductivity ( $\sigma$ ) for best quality ITO samples was found to be  $\sim 10^4 \text{ S/cm}$ .<sup>12</sup>

Recently, Yoo *et al.*<sup>13</sup> and He *et al.*<sup>14</sup> have reported both bulk and thin film samples of a diluted magnetic semiconductor—Fe and Cu codoped  $\text{In}_2\text{O}_3$  oxide. The solubility of Fe ions in the host compound was found to be around 20%, which is very high. In addition to that Ni-doped  $\text{In}_2\text{O}_3$  thin films were also found to be ferromagnetic at room temperature,<sup>15</sup> although the doping level of Ni ( $\sim 6 \text{ wt } \%$ ) was not as high as for samples reported in Ref. 13. Hong

*et al.*<sup>15</sup> showed that Ni is distributed uniformly throughout the film, which suggests that clustering of Ni particles in the samples is very unlikely. Hence, this fact gives a firm ground for assumption that observed ferromagnetism in their samples is rather intrinsic property of material. It is important to note that laser ablation technique used in Ref. 15 is a synthesis technique with nonequilibrium conditions. Therefore samples, prepared under equilibrium conditions, exhibiting same properties would confirm observed magnetic phenomena. In this letter we report on the observation of room temperature ferromagnetism in Ni-doped  $\text{In}_2\text{O}_3$  and ITO.

Polycrystalline samples of  $\text{In}_{2-x}\text{Ni}_x\text{O}_3$  and  $\text{In}_{2-x}\text{Ni}_x\text{Sn}_{0.02}\text{O}_3$  (1% Sn doping) were prepared by a conventional solid state synthesis technique.  $\text{In}_2\text{O}_3$  and  $\text{SnO}_2$  were factory prepared chemicals (high purity: 99.99%, Aldrich). Black NiO was prepared after decomposition of  $\text{Ni}(\text{OH})_2$  (high purity: 99.99%, Aldrich) in tube furnace at  $300 \text{ }^\circ\text{C}$  for 2 h in air. Starting materials were weighed and mixed in a mortar in corresponding ratios to obtain nominal chemical compositions for the final products. Mixed powders were calcined in an argon atmosphere at  $850 \text{ }^\circ\text{C}$  for 12 h. After that, the reacted powders were reground, pressed into the pellets, and fired at  $950 \text{ }^\circ\text{C}$  for 12 h in an argon atmosphere. The phases and crystal structure of samples were analyzed by means of x-ray diffraction technique (XRD) using  $\text{Cu } K\alpha$  irradiation (Mac Science; M03 XHF22). Figure 1 shows the XRD patterns of the pulverized pellets of  $\text{In}_{1.95}\text{Ni}_{0.05}\text{O}_3$  and  $\text{In}_{1.95}\text{Ni}_{0.05}\text{Sn}_{0.02}\text{O}_3$ . The observed diffraction patterns correspond to that of cubic  $\text{In}_2\text{O}_3$  phase. Lattice parameter  $a$  calculated from Rietveld refinements of the x-ray diffractograms showed some slight deviation from the literature data of  $a = 10.118 \text{ \AA}$ , i.e.,  $a(\text{In}_{1.95}\text{Ni}_{0.05}\text{O}_3) = 10.121 \text{ \AA}$  and  $a(\text{In}_{1.93}\text{Ni}_{0.05}\text{Sn}_{0.02}\text{O}_3) = 10.119 \text{ \AA}$ .

Transport properties were investigated using four point technique utilizing Physical Property Measuring System (PPMS, Quantum Design). Measurements were performed in a temperature range from 350 down to 5 K. Figure 2 represents the dependence of the electrical resistivity ( $\rho$ ) on temperature ( $T$ ) for both samples. Ni-doped  $\text{In}_2\text{O}_3$  shows a characteristic semiconducting behavior, while Ni-doped ITO clearly exhibits a metallic behavior with much lower  $\rho$ . The absolute value of  $\rho$  at 300 K of  $\text{In}_{1.95}\text{Ni}_{0.05}\text{O}_3$  was found to be  $\rho = 2 \Omega \text{ cm}$ , which is in a good agreement with published data for Ni-doped  $\text{In}_2\text{O}_3$  thin films.<sup>15</sup> At 300 K  $\text{In}_{1.93}\text{Ni}_{0.05}\text{Sn}_{0.02}\text{O}_3$  sample has  $\rho = 2.02 \times 10^{-2} \Omega \text{ cm}$ . A

<sup>a)</sup> Author to whom correspondence should be addressed; electronic mail: xiaolin@uow.edu.au

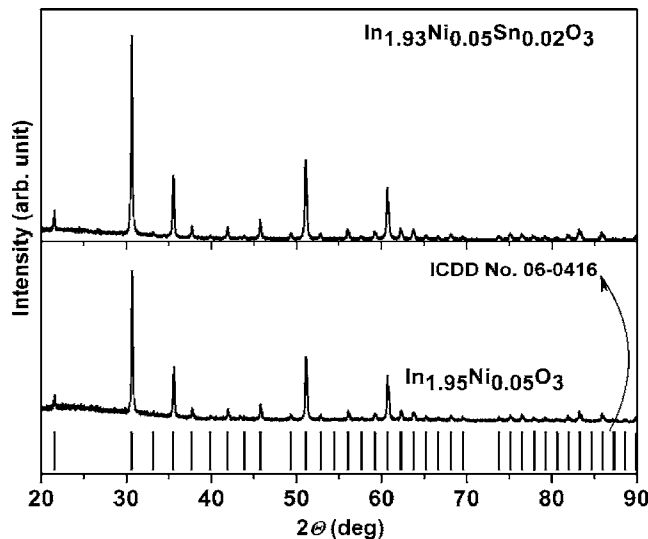


FIG. 1. X-ray powder diffraction patterns of pulverized  $\text{In}_{1.95}\text{Ni}_{0.05}\text{O}_3$  and  $\text{In}_{1.93}\text{Ni}_{0.05}\text{Sn}_{0.02}\text{O}_3$  pellets. The inset shows reference peaks for  $\text{In}_2\text{O}_3$  phase from ICDD Card No. 06-0416.

rather high resistivity of our Ni-doped ITO sample could be explained by probable porosity of the sample due to the preparation conditions (Ar atmosphere). Furthermore, as we can see from the inset in Fig. 2, there is a minimum point  $T=123$  K in the  $\rho$ - $T$  curve for Ni-doped ITO sample. One should consider two different mechanisms in two temperature ranges. When  $T > 123$  K, the temperature dependent electrical transport mechanism of the system should have negative temperature coefficient of resistivity (TCR). Then, if  $T < 123$  K, the TCR changes its value to +1. It is hard to explain what happens and why the sign of TCR changes. Ederth *et al.*<sup>16</sup> have argued that at temperatures above 123 K metallic behavior in electrical resistivity ( $\rho$ ) curves can be caused due to the sintering of conducting clusters, which lead to formation of conducting paths through the sample. Below  $T=123$  K the resistivity is dominated by ionized impurity scattering and thus TCR becomes positive.

Various electrical transport models were applied in order to understand which transport mechanism explains the  $\rho$ - $T$  data of  $\text{In}_{1.95}\text{Ni}_{0.05}\text{O}_3$  sample the best. Firstly hopping con-

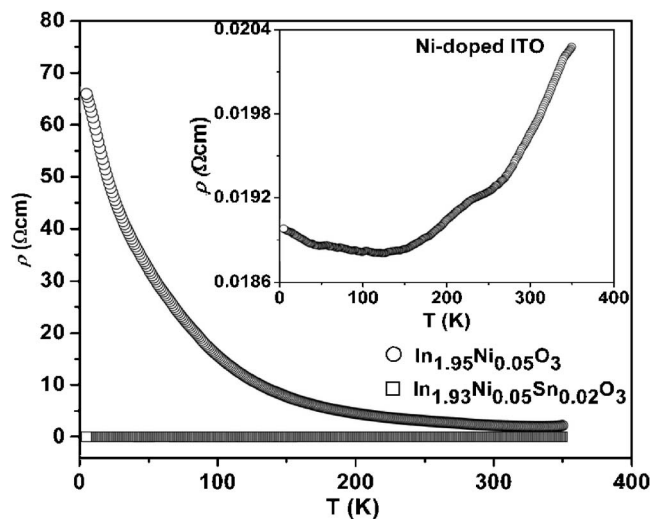


FIG. 2. Electrical resistivity ( $\rho$ ) vs temperature ( $T$ ) for  $\text{In}_{1.95}\text{Ni}_{0.05}\text{O}_3$  (open circle) and  $\text{In}_{1.93}\text{Ni}_{0.05}\text{Sn}_{0.02}\text{O}_3$  (open square). The inset represents magnified view of  $\rho$ - $T$  curve for Ni-doped ITO sample.

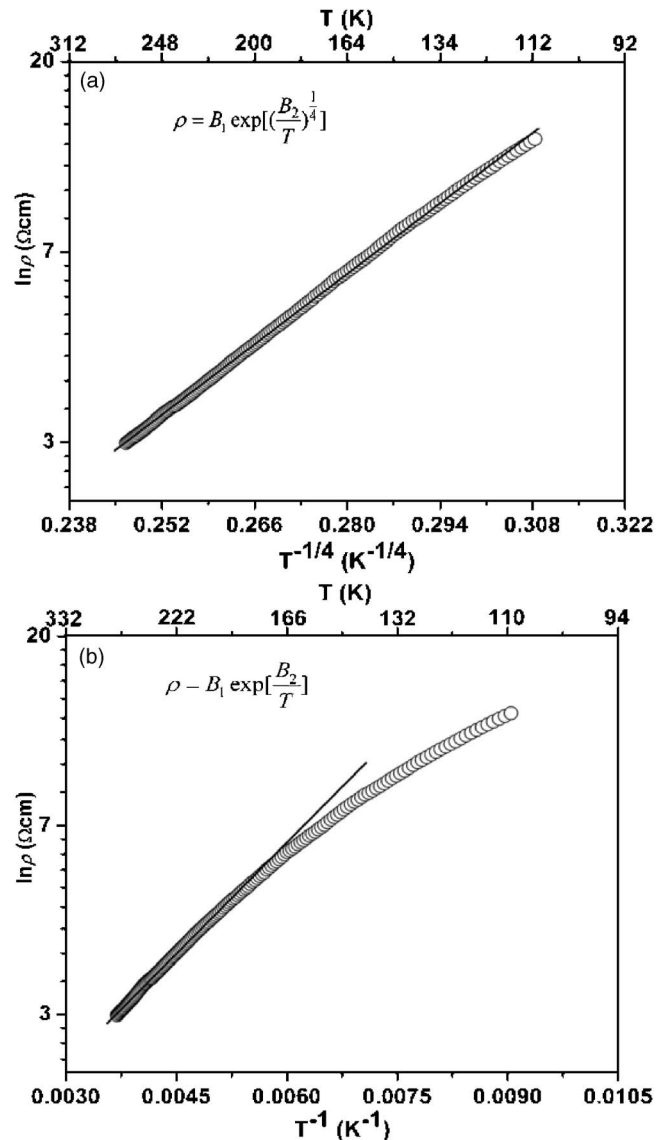


FIG. 3. Fittings of logarithm of electrical resistivity ( $\rho$ ) vs temperature ( $T$ ) for sample  $\text{In}_{1.95}\text{Ni}_{0.05}\text{O}_3$  applying (a) variable range hopping and (b) nearest neighbor hopping conduction models.

duction models were investigated. Generally hopping conduction can be represented by Eq. (1),

$$\rho = B_2 \exp \left[ \left( \frac{B_3}{T} \right)^{1/q} \right], \quad (1)$$

where  $B_1$ ,  $B_2$ , and  $q$  are constants, and  $T$  is temperature. A conduction mechanism dominated by hopping between localized states distributed randomly in the material [variable range hopping (VRH)] has a temperature dependence described by Eq. (1) with  $q=4$ . When  $q=1$  localized states are distributed in periodic array [nearest neighbor hopping (NNH)]. Secondly, a granular-metal (GM) system model was considered. In such system metallic grains are separated by thin insulating layers and  $q=2$ . Lastly, we have tried to fit our data with regard to degenerate semiconductor (DS) model, which is expressed by Eq. (2),

$$\rho(T) \propto T^{-3/2}. \quad (2)$$

For all of the mechanisms mentioned the fitted curves should be linear. Our investigation revealed that the broadest temperature range where  $\rho$ - $T$  curve can be linearly fitted corre-

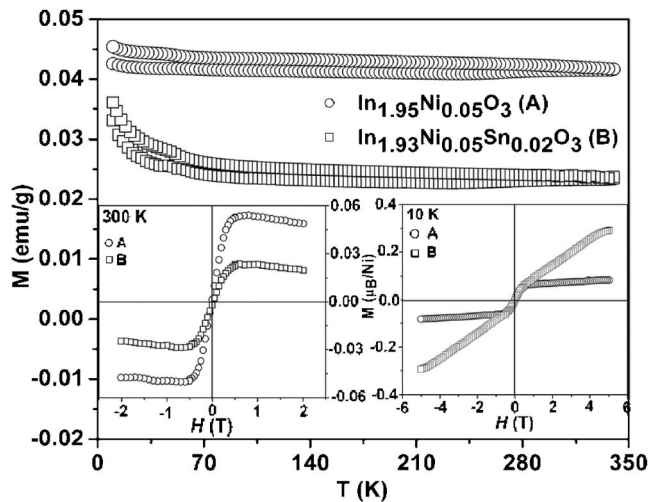


FIG. 4. Magnetization ( $M$ ) as a function of temperature ( $T$ ) for samples Ni-doped  $\text{In}_2\text{O}_3$  (open circle) and Ni-doped ITO (open square) under 2000 Oe applied magnetic field. Insets:  $M$ - $H$  loops of the same samples at 300 K (left) and 10 K (right).

sponds to that when  $q=4$ , i.e., VRH model [Fig. 3(a)]. Other curves showed large deviation from the linear fits in the same temperature range, e.g., NNH model [Fig. 3(b)]. Thus, VRH conduction mechanism explains transport properties of our Ni-doped  $\text{In}_2\text{O}_3$  sample the best.

The magnetization ( $M$ ) versus temperature ( $T$ ) data for Ni-doped  $\text{In}_2\text{O}_3$  and ITO samples are shown in Fig. 4. The zero field cooled (ZFC) measurements were done during warming in a field of 2000 Oe (Quantum Design, MPMS XL). Both samples were found to be ferromagnetic in the whole temperature range. The insets in Fig. 4 show magnetization ( $M$ ) versus applied magnetic field ( $H$ ) at 300 and 10 K. The maximal applied magnetic field varied from 2 to 5 T. Both samples show clear saturation magnetization ( $M_s$ ) at 300 K indicating high temperature ferromagnetism in the system. Observed  $M_s$  at 300 K was  $M_s=0.06\mu_B/\text{Ni}$  and  $M_s=0.03\mu_B/\text{Ni}$  for  $\text{In}_{1.95}\text{Ni}_{0.05}\text{O}_3$  and  $\text{In}_{1.93}\text{Ni}_{0.05}\text{Sn}_{0.02}\text{O}_3$ , respectively. The obtained  $M_s$  value for Ni-doped  $\text{In}_2\text{O}_3$  is smaller than  $M_s=0.7\mu_B/\text{Ni}$  at 300 K reported for Ni-doped  $\text{In}_2\text{O}_3$  thin films made by pulsed laser deposition (PLD).<sup>15</sup> On the other hand, our  $M_s$  values at 300 K for both compounds are well comparable to those reported for Mn-doped ITO thin films<sup>17</sup> and Co-doped  $\text{In}_2\text{O}_3$  thin films,<sup>18</sup>  $M_s=0.08\mu_B/\text{Mn}$  and  $M_s=0.05\mu_B/\text{Co}$ , respectively. Investigation of  $M$ - $H$  loops of the samples at 10 K showed that for Ni-doped  $\text{In}_2\text{O}_3$   $M$ - $H$  loop is still saturated and  $M_s=0.1\mu_B/\text{Ni}$ , while magnetic response of Ni-doped ITO sample does not have this trend anymore.

Different magnetic mechanisms might be responsible for observed magnetic phenomena in our samples.<sup>19</sup> Since our samples are highly conductive, the most “appropriate” model that would somehow support and explain the magnetism in our samples is carrier induced magnetism. It is known that carriers are donated by oxygen vacancies that act as shallow donors. Our samples were prepared under argon atmosphere, suggesting and thus supporting our speculation that the system must be rich in oxygen vacancies and thus itinerant carriers. Itinerant carriers coupled to local moments lead to the well-known Zener–Ruderman–Kittel–Kasuya–Yoshida (RKKY) mechanism of indirect magnetic interaction between the magnetic impurities with consequent induction of

ferromagnetic states. On the other hand,  $M$ - $H$  loops at 300 K (inset Fig. 4) showed that more conductive Ni-doped ITO sample has lower saturation magnetization, which contradicts the above mentioned model. It might be possible that lower portion of Ni ions contributes to the effective magnetic moment of the system. Other models, such as bound magnetic polarons (BMPs) and double exchange interaction, were also considered. In the former case, high conductivity of our samples contradicts requirements for BMP model to work. In the latter case, the probability of Ni being in multivalent state is very small, thus eliminating double exchange interaction mechanism from the list of choices as well.

In summary, polycrystalline Ni-doped  $\text{In}_2\text{O}_3$  and ITO samples were prepared. Both compounds were found to be ferromagnetic in the whole temperature range with saturation magnetizations ( $M_s$ ) at 300 K,  $M_s=0.06\mu_B/\text{Ni}$  and  $M_s=0.03\mu_B/\text{Ni}$  for  $\text{In}_{1.95}\text{Ni}_{0.05}\text{O}_3$  and  $\text{In}_{1.93}\text{Ni}_{0.05}\text{Sn}_{0.02}\text{O}_3$ , respectively.  $\text{In}_{1.95}\text{Ni}_{0.05}\text{O}_3$  transport properties measured showed a typical semiconducting behavior with  $\rho_{(300\text{ K})}=2\ \Omega\ \text{cm}$ , while Ni-doped ITO was found to be metallic with  $\rho_{(300\text{ K})}=2.06\times 10^{-2}\ \Omega\ \text{cm}$ . Analysis of the different conduction models suggested that electrical transport in our Ni-doped  $\text{In}_2\text{O}_3$  sample is best explained by variable range hopping (VRH) conduction mechanism.

One of the authors (X.L.W.) thanks the support from the Australian Research Council under Discovery Grant No. DP0 558 753. Another author (G.P.) thanks the Australian Government and the University of Wollongong for providing IPRS and UPA scholarships for his Ph.D. studies.

- <sup>1</sup>M. N. Baibich, J. M. Broto, A. Fert, F. N. Van Dau, and F. Petroff, *Phys. Rev. Lett.* **61**, 2472 (1988).
- <sup>2</sup>T. Dietl, H. Ohno, F. Matsukara, J. Cibert, and D. Ferrand, *Science* **287**, 1019 (2000).
- <sup>3</sup>K. Ueda, H. Tabata, and T. Kawai, *Appl. Phys. Lett.* **79**, 988 (2001).
- <sup>4</sup>K. P. Bhatti, S. Chaudhary, D. K. Pandya, and S. C. Kashyap, *Solid State Commun.* **136**, 384 (2005).
- <sup>5</sup>C. B. Fitzgerald, M. Venkatesan, J. G. Lunney, L. S. Dorneles, and J. M. D. Coey, *Appl. Surf. Sci.* **247**, 493 (2005).
- <sup>6</sup>A. S. Risbud, N. A. Spaldin, Z. Q. Chen, S. Stemmer, and R. Seshadri, *Phys. Rev. B* **68**, 205202 (2003).
- <sup>7</sup>J. Alaria, P. Turek, M. Bernard, M. Bouloudenine, A. Berbadj, N. Brihi, G. Schmerber, S. Colis, and A. Dinia, *Chem. Phys. Lett.* **415**, 337 (2005).
- <sup>8</sup>S. Kolesnik, B. Dabrowski, and J. Mais, *J. Appl. Phys.* **95**, 2585 (2004).
- <sup>9</sup>S. B. Ogale, R. J. Choudhary, J. P. Buban, S. E. Lofland, S. R. Shinde, S. N. Kale, V. N. Kulkarni, J. Higgins, C. Lanci, J. R. Simpson, N. D. Browning, S. D. Sarma, H. D. Drew, R. L. Greene, and T. Venkatesan, *Phys. Rev. Lett.* **91**, 077205 (2003).
- <sup>10</sup>J. H. Kim, H. Kim, D. Kim, A. E. Yhm, and W. K. Choo, *J. Eur. Ceram. Soc.* **24**, 1847 (2004).
- <sup>11</sup>P. Nath and R. F. Bunshah, *Thin Solid Films* **80**, 63 (1980).
- <sup>12</sup>K. Utsumi, O. Matsunaga, and T. Takahata, *Thin Solid Films* **334**, 30 (1998).
- <sup>13</sup>Y. K. Yoo, Q. Xue, H. C. Lee, S. Cheng, X. D. Xiang, G. F. Dionne, S. Xu, J. He, Y. S. Chu, S. D. Preite, S. E. Lofland, and I. Takeuchi, *Appl. Phys. Lett.* **86**, 042506 (2005).
- <sup>14</sup>J. He, S. Xu, Y. K. Yoo, Q. Xue, H. C. Lee, S. Cheng, X. D. Xiang, G. F. Dionne, and I. Takeuchi, *Appl. Phys. Lett.* **86**, 052503 (2005).
- <sup>15</sup>N. H. Hong, J. Sakai, N. T. Huong, and V. Brizé, *Appl. Phys. Lett.* **87**, 102505 (2005).
- <sup>16</sup>J. Ederth, P. Johansson, G. A. Niklasson, A. Hoel, A. Hultåker, P. Heszler, C. G. Granqvist, A. R. van Doorn, M. J. Jongerius, and D. Burgard, *Phys. Rev. B* **68**, 155410 (2003).
- <sup>17</sup>J. Philip, N. Theodoropoulou, G. Berera, and J. S. Moodera, *Appl. Phys. Lett.* **85**, 777 (2004).
- <sup>18</sup>N. H. Hong, J. Sakai, N. T. Huong, and V. Brizý, *J. Magn. Magn. Mater.* **302**, 228 (2006).
- <sup>19</sup>M. J. Calderon and S. Das Sarma, e-print cond-mat/0603182.